International Journal of Engineering Trends and Technology
ISSN: 2231–5381 / https://doi.org/10.14445/22315381/IJETT-V72I8P118

Volume 72 Issue 8, 174-185, August 2024

Original Article

A Study on Design of Yaw Gearbox for Large-Capacity Wind Turbines

Back-Hun Lee[1], Jae-Sin Lee[1], Min-Woo Kim[1], Young-Kuk Kim[1], Yu-Jin Jeong[1], Hyoung-Woo Lee[2*]

[1]*Department of Mechanical Engineering, Jungwon University, Republic of Korea, Chungbuk.*
[2]*Department of Unmanned Aeromechanical Engineering, Jungwon University, Republic of Korea, Chungbuk.*

[*]*Corresponding Author : leehwoo@jwu.ac.kr*

Received: 25 April 2024 Revised: 11 July 2024 Accepted: 30 July 2024 Published: 28 August 2024

Abstract *- This paper conducted structural analysis and vibration characteristic analysis to verify the stability of yaw gearboxes for large-capacity wind turbines. For the carriers and housing of the yaw gearbox designed for large-scale wind turbines, structural analysis was performed based on the Load Duration Distribution (LDD) data for extreme load conditions. The results confirmed that all parts met the safety factor of 1.3 or higher, as specified in IEC 61400-1. Additionally, eigenvalue analysis and critical speed analysis were conducted using MASTA11 for the planetary gear train vibration model. The findings demonstrated that within the operating speed range, there was no resonance for mass imbalance or gear mesh frequency.*

Keywords *- Wind turbine, Planetary gear train, Structural analysis, Vibration, Yaw gearbox.*

1. Introduction

The yaw system in wind power generation aligns the rotor and nacelle with the direction of the wind, optimizing the efficiency of the wind power system and reducing the fatigue loads acting on the entire system. If there is a yaw error, where the wind direction does not align perfectly with the main axis, it can not only decrease the output of the wind turbine but also shorten its lifespan due to abnormal loads. When the rotating blades of the wind turbine are not perpendicular to the wind, a yaw error occurs. This means that some of the energy contained in the wind passes through the rotational plane of the turbine [1]. The demand for wind turbine gearboxes to be more compact, lighter, quieter, more efficient, and have a longer lifespan is increasing. To meet these demands, the planetary gear train structure is widely used. In a planetary gear train, power is transmitted by dividing the input power among several planetary gears. Since the input and output shafts are coaxially aligned, this allows for designs that are compact and lightweight. In addition, since many components can be designed to be smaller, the pitch line velocity of the gears is reduced, which is beneficial in terms of efficiency and noise. Moreover, because gear reducers have a high reduction ratio, the gears must perform effectively even under load [2~4]. Research on planetary gear trains includes the following: A. E. Ikpe simulated the sun gear and carrier of a two-stage planetary gear train for wind turbines, analyzing stress, strain, and overall deformation. V. L, Jantara Junior presented various challenges that must be addressed to increase the operational lifespan of wind turbine gearboxes significantly. H. Yin and A. Mohsine performed finite element analysis on planetary gear sets [5-8]. Smota Pawar and Avinash Lavnis conducted finite element analysis on gearbox housings, and Josef Brousek and Robert Vozenilek did the same for gearbox housings in battery electric vehicles. M.aulik M. Patel and Neha B. Joshi carried out fatigue analysis on gearbox carriers to analyze stress distribution [9]. F.K. Choy and Y.F. Ruan presented a comprehensive approach to analyzing the dynamic behavior of multi-stage gear transmission systems, including the effects of vibrations induced by the gearbox and rotor mass imbalance. They developed a combined approach using modal synthesis and the finite element method to analyze the mechanics of gear systems [10-11]. D.H. Lee, I. S. Youn, and G. J. Cheon calculated the eigenvalues and eigenvectors for the gearbox of a planetary gear type reducer and conducted a modal analysis to validate the finite element model [12]. This paper verified the stability of yaw gearboxes for large-scale wind turbines through structural analysis and critical speed analysis.

The yaw gearbox for wind turbines was designed with a target safety factor of 1.3 or higher, as specified in IEC 61400-1 for wind turbine components. Using MASTA11, eigenvalue analysis and critical speed analysis were performed on the planetary gear train vibration model to check for resonance within the operational speed range. By connecting the gear train model of the yaw gearbox for large-capacity wind turbines and the housing carrier with a substructural synthesis method, the critical speed analysis was performed about Mass imbalance and Gear Mesh Frequency to apprehend the mode shape and natural frequency. As a result of the critical speed

analysis, the safety verification was performed by checking whether resonance occurred within the operating speed range.

2. Structural Analysis of Yaw Gearbox

2.1. Finite Element Analysis of Housing

As shown in Figure 1, the housing of the wind turbine Yaw gearbox is composed of components such as the motor flange, flange, ring gears of a four-stage planetary gear system, and output housing. The ring gear receives rotational force from the planetary gear and transmits this load to the connected flange. The output housing is attached to the wind turbine's nacelle and supports the load of the bearings that support the output shaft. Figure 1 shows the finite element analysis model of a wind turbine yaw gearbox housing. Finite element analysis is a stress analysis method that virtually divides a structure into finite-sized elements and analyzes the structure as an assembly of these elements. The finite element model was created using ANSYS 21, and bolts were excluded from the analysis model due to the high potential for stress concentration. The model consists of 8,524,118 nodes and 2,320,045 elements. The material properties of each component of the wind turbine yaw gearbox housing are presented in Table 1.The boundary conditions for the finite element model of the housing are shown in Figure 2. In actual use, the yaw gearbox for wind turbines is attached to the nacelle and connected through the output housing and bolts. The output pinion of the yaw gearbox meshes with the yaw bearing to adjust the direction of the wind turbine's nacelle. Fixed support constraints were applied to the points where the motor flange and the motor are fastened and where the Nacelle and output housing are bolted together.

Table. 1 Material properties of housing components of the yaw gearbox for wind turbines

Material	Young's Modulus [GPa]	Poisson's Ratio	Yield Strength [MPa]	Tensile Strength [MPa]
FCD450	173	0.3	250	400
FCD600	173	0.3	370	600
SCM440	207	0.3	835	980

Fig. 1 Finite element analysis model of yaw gearbox housing for wind turbines

Fixed Support **Compression-Only Support**

Fig. 2 Boundary conditions of finite element analysis of housing

Table 2. Load conditions of yaw gearbox housing for finite element analysis

Part	Value
1st Ring Gear	746,870 N·mm
2nd Ring Gear	4,896,200 N·mm
3rd Ring Gear	18,151,000 N·mm
4th Ring Gear	85,558,000 N·mm
Bearing Load 1	542,790 N
Bearing Load 2	1.432,800 N

For the part where the nacelle supports the output housing, compression-only support was applied, which allows for deformation under compression but not under tension, to perform the finite element analysis. The load conditions are shown in Figure 3.

When applying load conditions to the teeth of the ring gear, there is a potential for stress concentration at the root of the tooth where the load is applied. As such, after designating the holes where each ring gear and flange are bolted together, a remote point was set up. Finite element analysis was conducted by applying a bearing load to the surface where the main bearing of the output housing is located. The load carried out with the largest load from the conditions is shown in Table 2. Finite element analysis was Load Duration Distribution (LDD) data.

Torque was applied to the 1st to 4th ring gears, and bearing loads to the area where the bearings of the output housing are located. The finite element results for the housing of the yaw gearbox for wind turbines are presented in Figure 4. The highest stress occurred in the output housing at the location where bearing load 2 was applied, showing a maximum stress of 214 MPa. Table 3 presents the safety factor, calculated based on the yield strength of the housing material and the maximum stress observed in each component. The lowest safety factor of 1.7 was observed in the output housing.

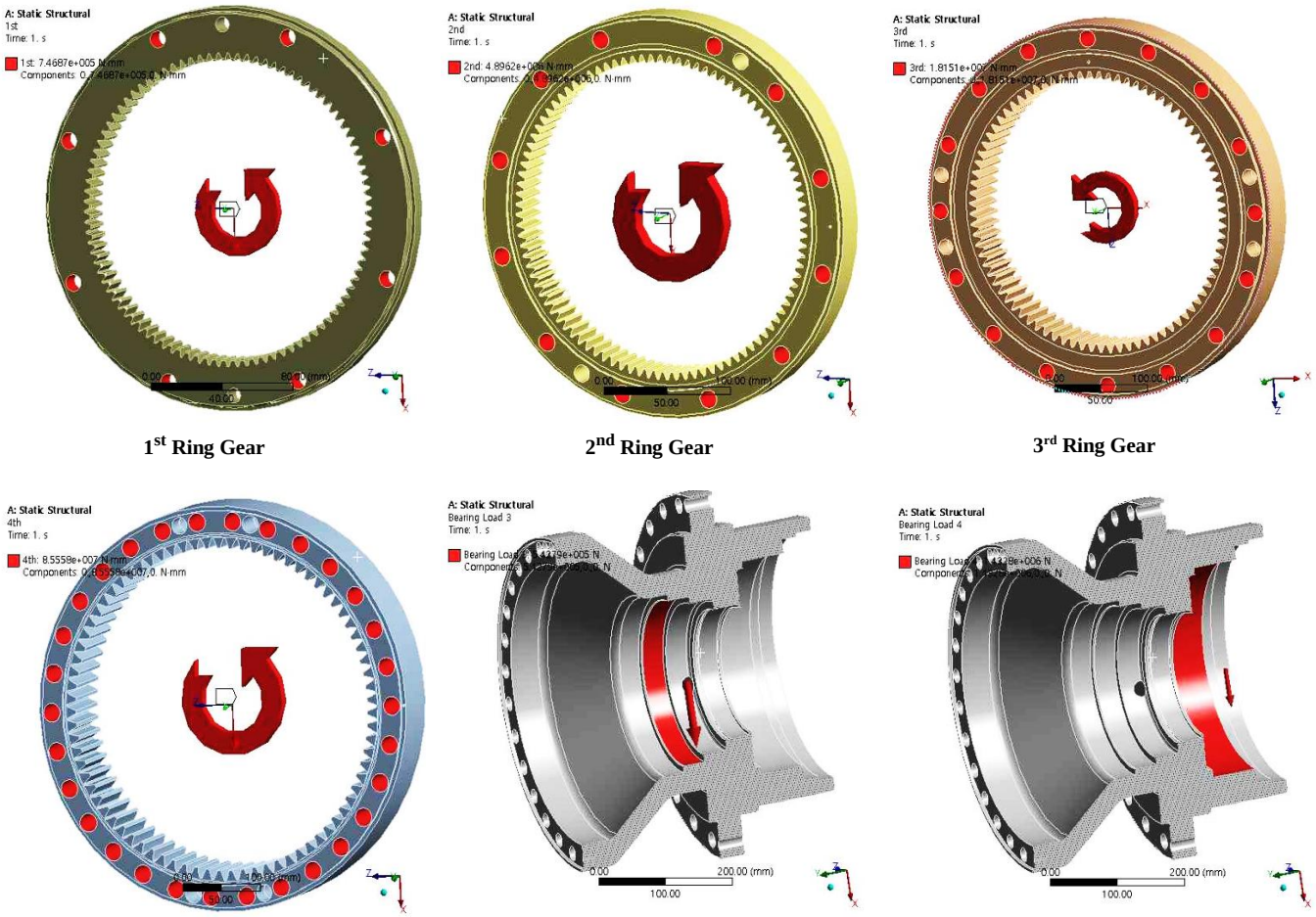

1st Ring Gear | 2nd Ring Gear | 3rd Ring Gear

4th Ring Gear | Bearing Load 1 | Bearing Load 2

Fig. 3 Load conditions of housing

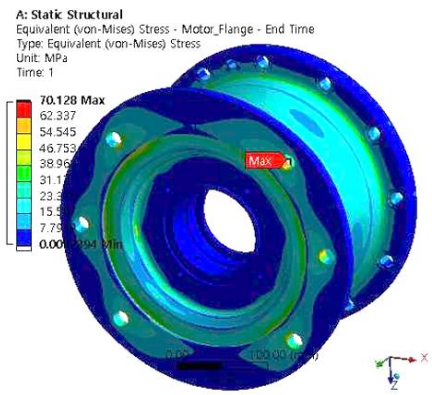

Motor Flange

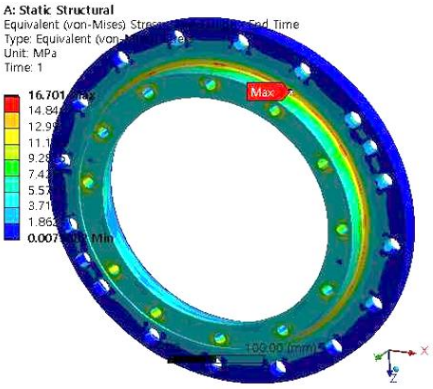

2nd Flange

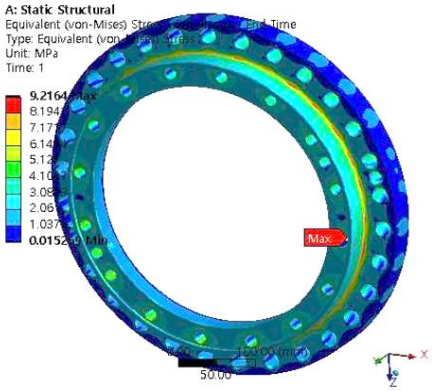

3rd Flange

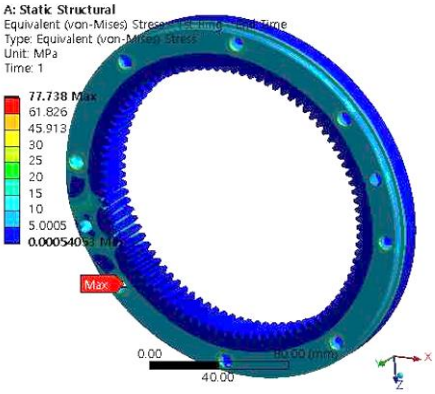

1st Ring Gear

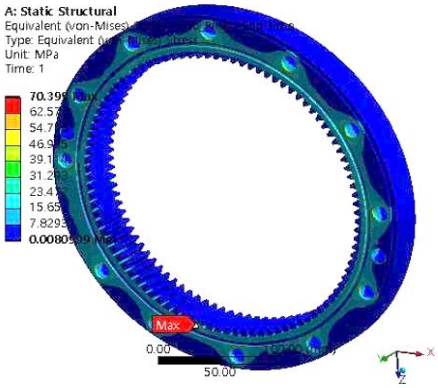

2nd Ring Gear

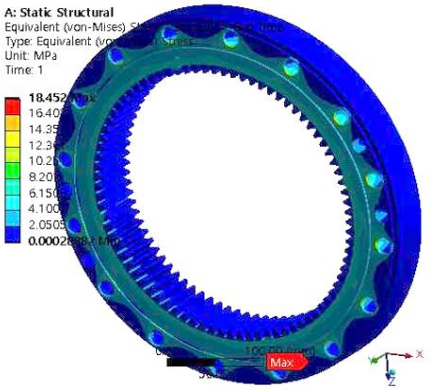

3rd Ring Gear

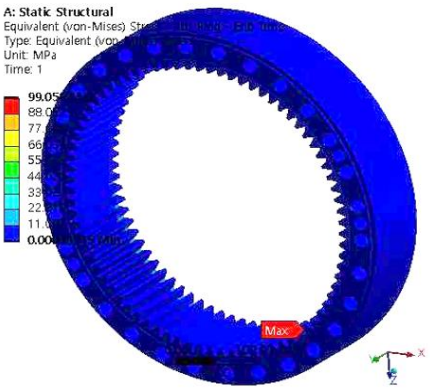

4th Ring Gear

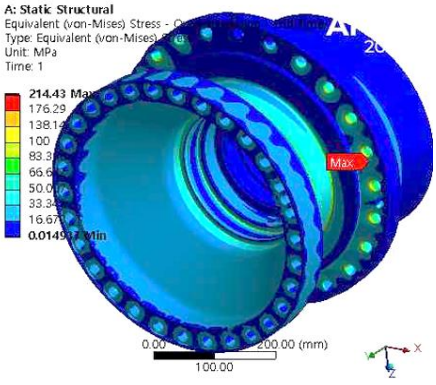

Output Housing

Fig. 4 Results of finite element analysis for yaw gearbox housing

Table 3. Safety factors of each housing part of the yaw gearbox for wind turbines

Part	Yield Strength [MPa]	Maximum Stress [MPa]	Safety Factor
Motor Flange	250	70.12	3.6
2nd Flange	250	16.7	15.0
3rd Flange	250	9.21	27.1
Output Housing	370	214.43	1.7
1st Ring Gear	835	77.73	10.7
2nd Ring Gear	835	70.39	11.9
3rd Ring Gear	835	18.45	45.3
4th Ring Gear	835	99.5	8.4

1st Carrier **2nd Carrier**

3rd Carrier **4th Carrier**

Fig. 5 Finite element analysis model of yaw gearbox carriers

Table. 4 Mechanical properties of yaw gearbox carrier materials for wind turbines

Carrier	Material	Young's Modulus [GPa]	Poisson's ratio	Yield Strength [MPa]	Tensile Strength [MPa]
1st	S45C	207	0.3	490	686
2nd	FCD 450	173	0.3	250	400
3rd					
4th	FCD 600	173	0.3	370	600

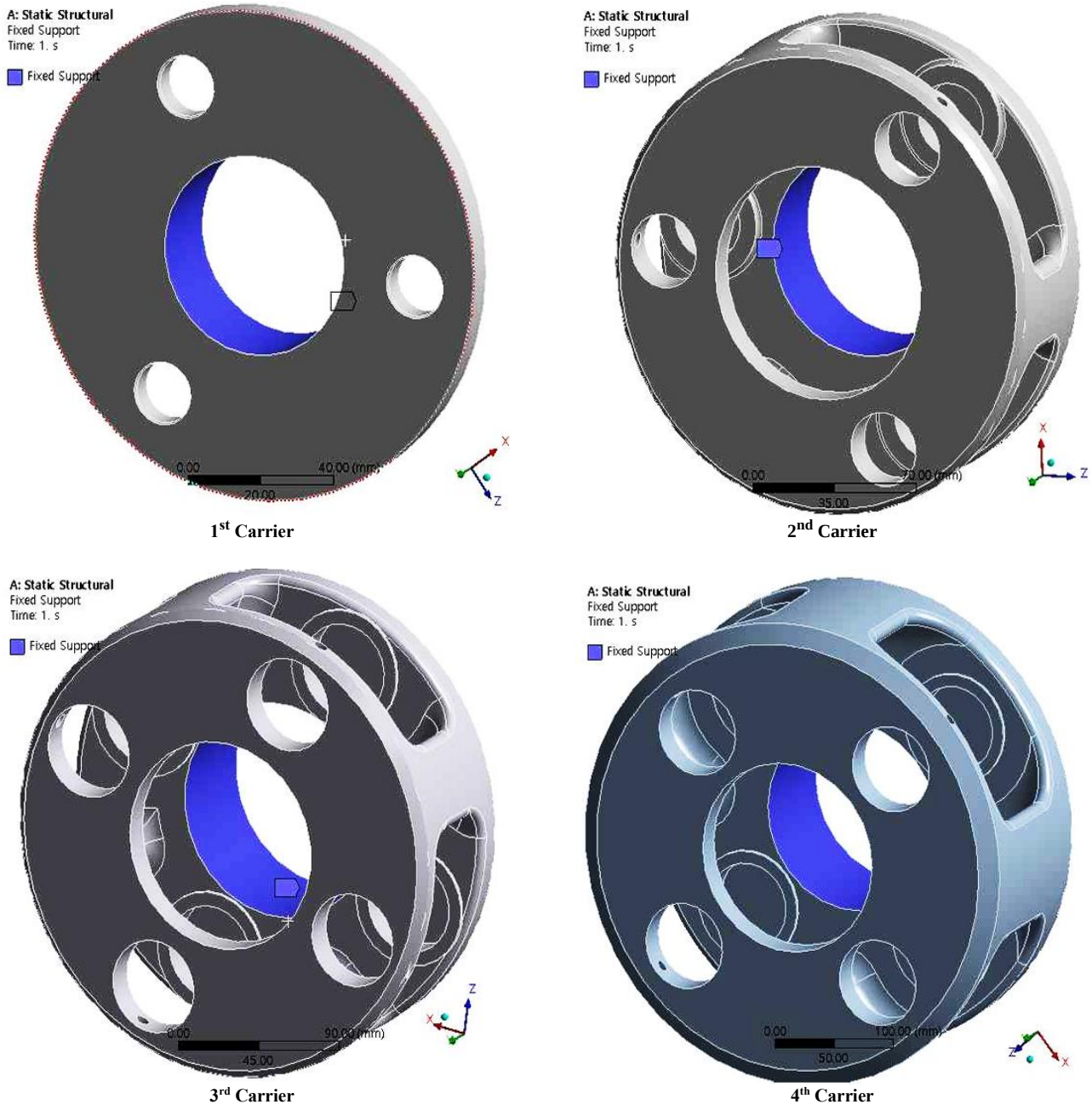

Fig. 6 Boundary conditions of yaw gearbox carriers

2.2. Finite Element Analysis of Carriers

The yaw gearbox for wind turbines features a four-stage planetary gear system, which includes a total of four carriers. The ring gear is fixed, and the first sun gear receives rotational power from the motor. As the power is transmitted to the planetary gears, the rotational speed is reduced, thereby strengthening the rotational force. Subsequently, the carrier connected to the planetary gears transfers this rotational force to the second sun gear, which then passes the force to the second planetary gears, further reducing the rotational speed and strengthening the force. Finally, the rotational force from the fourth carrier is transmitted to the output shaft. The finite element analysis model of the carriers of the yaw gearbox for wind turbines is shown in Figure 5. Using ANSYS 21, finite element analysis was performed, and the gear teeth of the carrier connected to the next sun gear or output shaft were removed to minimize the occurrence of stress-based singular solutions. The first carrier has 582,820 nodes and 146,223 elements. The second carrier has 1,187,263 nodes and 326,998 elements. The third carrier has 1,223,601 nodes and 337,226 elements. The fourth carrier has 1,525,024 nodes and 424,373 elements.

The mechanical properties of the materials used for the carriers in the planetary gear system of the yaw gearbox for wind turbines are presented in Table 4. The first carrier is made of S45C, which is used for parts requiring mechanical strength. FCD450, used for the flanges of the housing, is employed for the second and third carriers, while FCD600, used for the output housing, is utilized for the fourth carrier.

The boundary conditions for the finite element analysis of the carriers are shown in Figure 6. For the first carrier, the gear teeth of the spline section, which transmits rotational force to the next stage, were removed, and fixed support conditions were applied. Similarly, for the second to fourth carriers, the gear teeth of the splines were also removed, and finite element analysis was performed after entering the fixed support conditions. The load conditions for the finite element analysis of the carriers are displayed in Figure 7. After selecting the area where the pin connects, a remote point was set up, and the largest load from the Load Duration Distribution (LDD) data was applied for the finite element analysis.

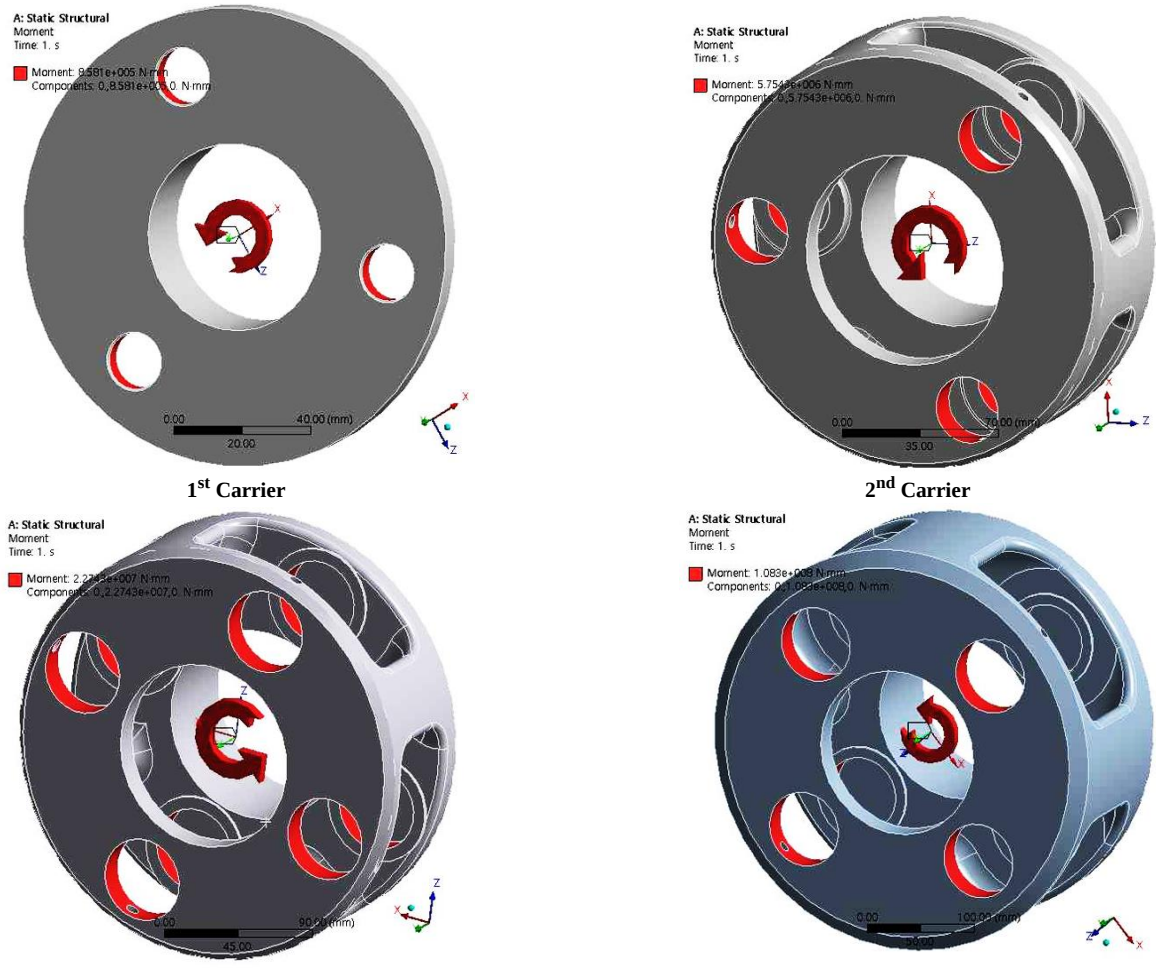

Fig. 7 Load conditions of yaw gearbox carriers

Table 5. Load values of yaw gearbox carriers

Part	Value [N·mm]
1st Carrier	858,097
2nd Carrier	5,754,305
3rd Carrier	22,743,212
4th Carrier	108,301,015

Table 5 presents the load values for the load conditions of the yaw gearbox carriers. For the finite element analysis of the carriers in the yaw gearbox for wind turbines, the largest load from the Load Duration Distribution (LDD) data was applied. The load condition value for the first carrier is 858,097 N·mm, and the largest load is applied to the fourth carrier, which is 108,301,015 N·mm. The results of the finite element analysis for the carriers of the yaw gearbox for wind turbines are shown in Figure 8. Among the carriers, the highest stress occurred in the fourth carrier at the pin connection, where the load value was entered via a remote point, registering 245.06 MPa. The lowest stress was observed in the first carrier at the pin connection, where the load value was entered via a remote point, with a value of 103.81 MPa. Table 6 calculates the safety factors using the yield strength of the housing material and the maximum stress observed in each part. The highest safety factor was 4.72 for the first carrier, and the lowest was 1.51 for the fourth carrier.

Table 6. The safety factor of year gearbox carriers for wind turbines

Part	Yield Strength [Mpa]	Maximum Stress [Mpa]	Safety Factor
1st Carrier	490	103.81	4.72
2nd Carrier	250	140.28	1.78
3rd Carrier	250	162.98	1.53
4th Carrier	370	245.06	1.51

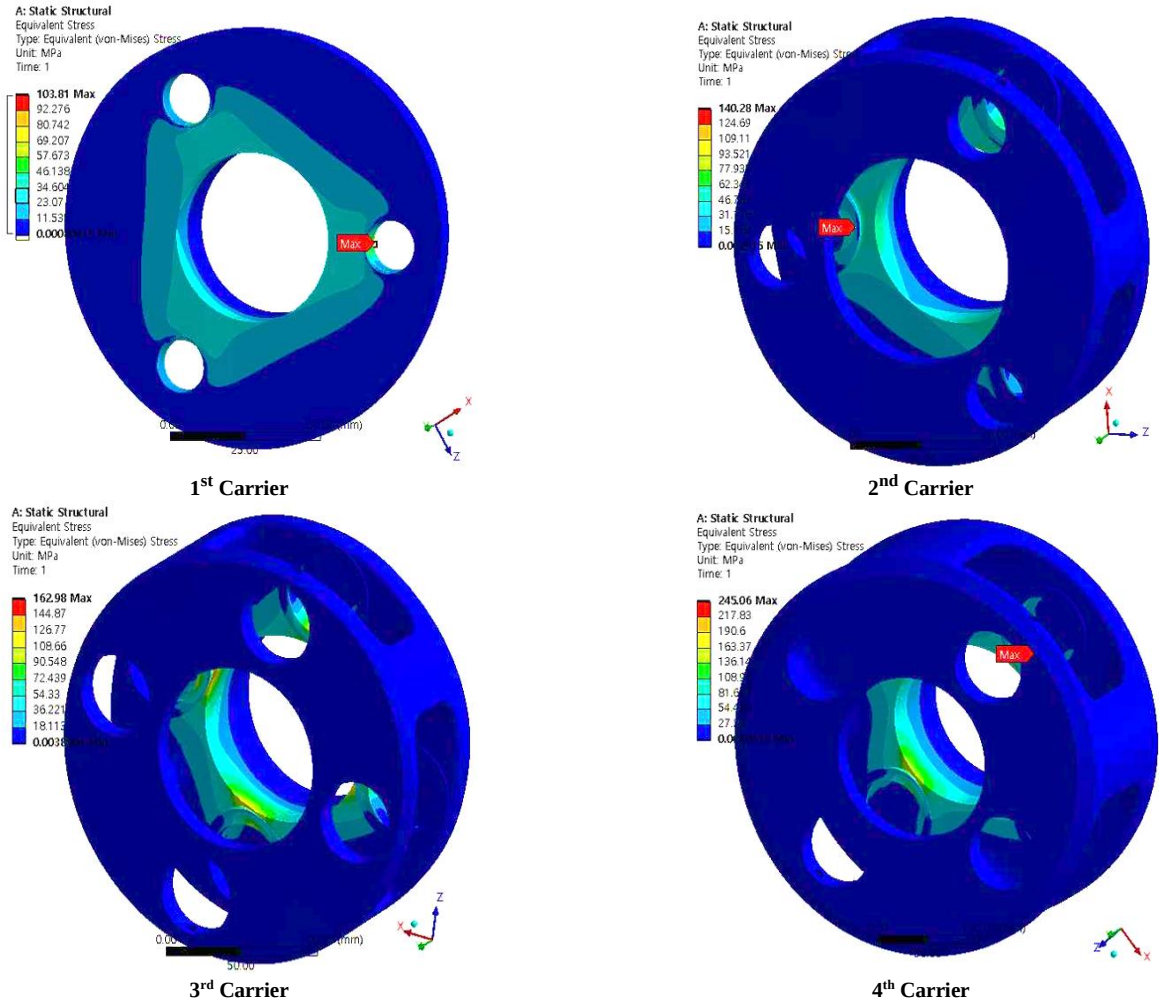

1st Carrier 2nd Carrier

3rd Carrier 4th Carrier

Fig. 8 Results of finite element analysis for yaw gearbox carriers

3. Analysis of Vibration Characteristics of Yaw Gearbox for Wind Turbines

The gear train of the yaw gearbox for wind turbines is a four-stage planetary gear system. In this system, the planetary gears are mounted on the carriers and rotate around the central sun gear, and the ring gears enclose the planetary gears. This arrangement, consisting of multiple planetary gears, has the advantage of distributing the load effectively, which extends the lifespan and allows for a variety of gear ratios in a confined space. The specifications of the planetary gear system for modal analysis are shown in Table 7. The first and second stages have three pinion gears each, while the third and fourth stages have four each. The pressure angle is 20° for the first stage and 25° for stages two to four. The model for modal analysis was modelled using MASTA11, as shown in Figure 9.

The modal analysis involves determining the natural frequencies and mode shapes of the planetary gear train. The general equation for modal analysis is given in Equation (1).

$$[M]\ddot{x} + [K]x = 0 \tag{1}$$

$$x = \varphi_i \cos(\omega_i t) \tag{2}$$

Equation 3 is obtained by substituting Equation (2) into Equation (1). In modal analysis, this determinant is used to derive the natural frequency and mode shape.

$$([K] - \omega_i{}^2[M]\varphi_i) \tag{3}$$

The assumption in Equation (3) is as follows: [K] and [M] are constants representing the stiffness and mass matrices of the entire system, respectively.

Table 7. Specifications of four-stage planetary gear system

Stage	1			2			3			4		
	S	P	R	S	P	R	S	P	R	S	P	R
Planetary Gear	3			3			4			4		
Module	1.75			2.5			3.5			5		
Pressure Angle [°]	20			25			25			25		
Number of Teeth	14	39	94	17	39	97	21	30	83	21	28	79
Center Distance [mm]	47.6			71.7			91.4			125.5		
Reduction Ratio	7.714			6.706			4.952			4.762		

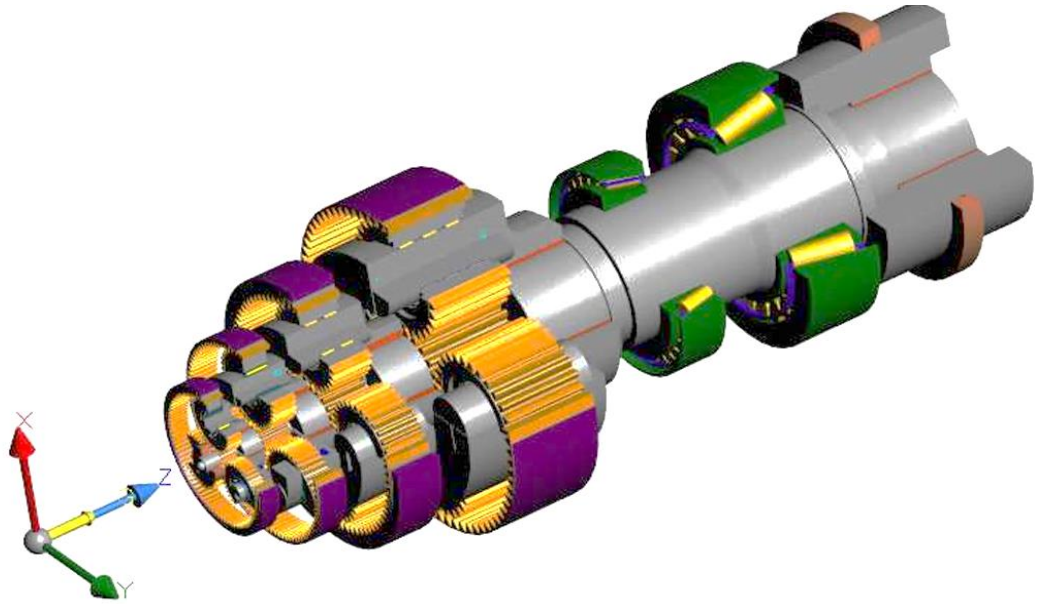

Fig. 9 Vibration model of yaw gearbox for wind turbines

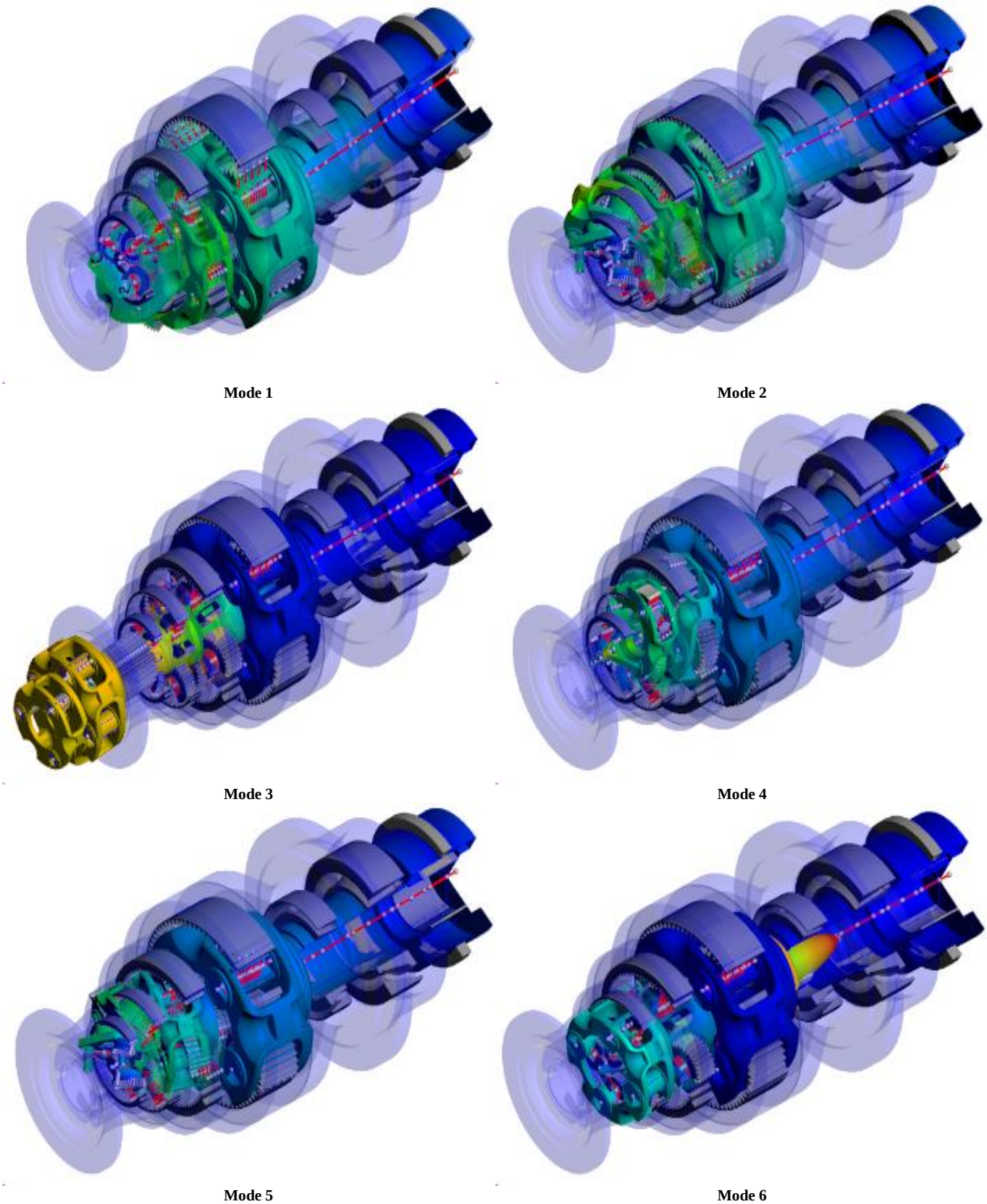

Mode 1 **Mode 2**

Mode 3 **Mode 4**

Mode 5 **Mode 6**

Fig. 10 Mode analysis results

Table. 8 Natural frequency analysis

Mode	Natural Frequency [Hz]
1	114.186
2	115.787
3	230.232
4	308.917
5	309.633
6	388.656

Table 9. Excitation frequency ratio of yaw gearbox for wind turbines

Excitation Source	Excitation Frequency Ratio		
	Carrier	Sun	Planetary
Mass Imbalance	1st	1X	0.13X
	2nd	0.13X	0.019X
	3rd	0.019X	0.004X
	4th	0.004X	0.001X
Gear Mesh Frequency	1st	14X	
	2nd	2.204X	
	3rd	0.406X	
	4th	0.082X	

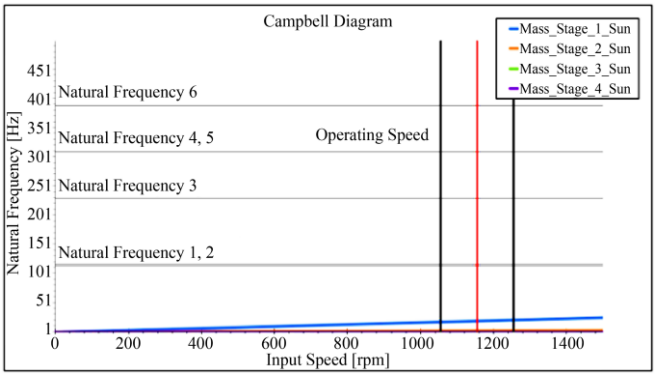

Fig. 11 Campbell diagram of mass imbalance

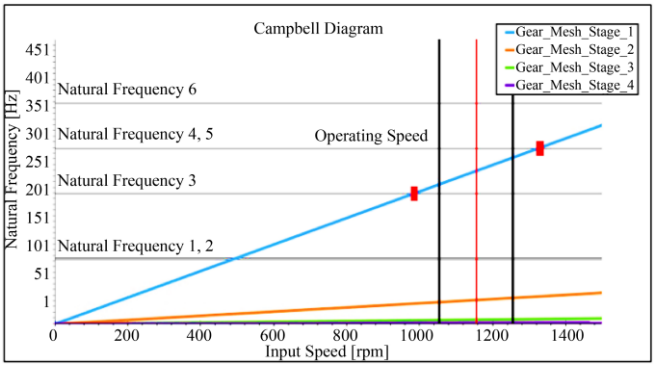

Fig. 12 Campbell diagram of gear mesh frequency

Figure 10 shows the results for the mode shapes, illustrating the vibration patterns of each natural frequency. The first and second modes showed the largest deformations in the carriers of stages 1-4, while the fourth and fifth modes showed deformations in the carriers of stages 1-3. The third and sixth modes showed significant axial deformations in the third-stage carrier. Table 8 presents the results of the natural frequency analysis.

Excitations acting on wind power systems include those caused by rotational imbalances, tooth contact errors at gear interfaces, tooth pitch errors, and excitation sources arising from wind loads applied to blades. Additionally, there are excitations due to temporal changes in the tooth stiffness coefficient. [13]Critical speed analysis was conducted by calculating the excitation frequency ratio for mass imbalance and gear mesh frequency. Mass imbalance, the most common excitation in rotating machinery, occurs when the center of mass does not coincide with the axis of rotation. Gear mesh frequency excitation arises from vibrations caused when the teeth of meshing gears collide.

Table 9 presents the excitation frequency ratios for mass imbalance and gear mesh frequency excitation sources. X represents the rotational speed of the input shaft, where 1X is the vibration frequency ratio of the first sun gear. The vibration frequency ratio of the first planetary gear is calculated based on the reduction ratio between the sun gear and the carrier. The excitation frequency ratio of gear mesh frequency is calculated by multiplying the number of teeth on the sun gear by the excitation frequency ratio of the mass imbalance for that stage.

In a Campbell diagram, the X-axis represents rpm, and the Y-axis represents frequency. The natural frequencies are shown on the Y-axis, and the excitation frequency ratio is displayed as a straight line. Resonance occurs when the lines of natural frequency and excitation frequency ratio intersect within the operating speed range. The operating speed of the yaw gearbox for wind turbines is set at 1155 rpm, and by calculating ± 100 rpm, the range was set as 1055 to 1255 rpm.

Figures 11 and 12 show the Campbell diagrams 1055 to 1255 rpm. Figures 11 and 12 show the Campbell diagrams for mass imbalance and gear mesh frequency. Within the operating speed range, the excitation frequency ratio does not coincide with the natural frequency, indicating no resonance.

4. Conclusion

This paper conducted finite element analysis on the carriers and housing of the yaw gearbox for large-capacity wind turbines using the largest load from Load Duration Distribution (LDD) data. Boundary conditions were applied to the bolt holes connecting the housing to the motor, and the nacelle, as well as the areas held by the nacelle. For the finite element analysis, extreme loads were applied using a remote point at the bolt holes of ring gears, and bearing loads were applied at the locations of the bearings. The carrier had gear teeth removed at the spline locations connecting to the next sun gear, and extreme loads were applied to remote points at the pin connections.

As a result, all components of the wind turbine met the safety factor of 1.3, as specified in IEC 61400-1. Modal analysis and critical speed analysis were also performed for the largest load in the LDD data. Within the operating speed range, critical speeds did not exist.

Acknowledgements

This work was supported by the Korea Institute of Energy Technology Evaluation and Planning (KETEP) of the Republic of Korea (No.20213030020020).

References

[1] Hyun-Joo Lee, Won-Ho Choi, and Kyoung Min Ahn, "Design of Yaw System of Wind Turbin," *Korean Society for New and Renewable Energy*, pp. 277-280, 2006. [Google Scholar] [Publisher Link]

[2] KwangMin Kim, MyungHo Bae, and YonSang Cho, "Fatigue Strength Analysis of Complex Planetary Gear Train of the Pitch Drive System for Wind Turbines," *Korean Tribology Society*, vol. 37, no. 2, pp. 48-53, 2021. [CrossRef] [Google Scholar] [Publisher Link]

[3] Jeong-gil Kim et al., "A Study on the Effect of Manufacturing Errors on the Load Sharing of the Planetary Geartrain," *Journal of the Korean Society for Agricultural Machinery*, vol. 24, no. 2, 2019. [Google Scholar] [Publisher Link]

[4] Lim Ki-ryong et al., "Study on Tooth Optimization for Angle of Elevation Drive Reducer," *The Korean Society of Manufacturing Process Engineers Proceedings of the KSMPE Conference*, 2016. [Google Scholar] [Publisher Link]

[5] Aniekan Essienubong Ikpe, Ekom Mike Etuk, and Azum Uwarisi Adoh, "Modelling and Analysis of 2-Stage Planetary Gear Train for Modular Horizontal Wind Turbine Application," *Journal of Applied Research on Industrial Engineering*, vol. 6, no. 4, pp. 268-282, 2019. [CrossRef] [Google Scholar] [Publisher Link]

[6] V.L. JantaraJunior et al., "Evaluating the Challenges Associated with the Long-Term Reliable Operation of Industrial Wind Turbine Gearboxes," *International Conference on Materials Engineering and Science*, Istanbul, Turkey, vol. 454, pp. 1-8, 2018. [CrossRef] [Google Scholar] [Publisher Link]

[7] Huabing Yin et al., "The Load Sharing Structure Design and FE Analysis of Planetary Gearbox With Flexible Pin," *2021 2nd International Conference on Mechatronics Technology and Intelligent Manufacturing*, Hangzhou, China, vol. 2029, pp. 1-6, 2021. [CrossRef] [Google Scholar] [Publisher Link]

[8] Abdellah Mohsine, El Mostapha Boudi, and Abdellatif El Marjani, "Modeling and Structural Analysis of Planetary Gear of a Wind Turbine," *2016 International Renewable and Sustainable Energy Conference*, Marrakech, Morocco, pp. 462-466, 2016. [CrossRef] [Google Scholar] [Publisher Link]

[9] Maulik M. Patel, and Neha B. Joshi, "Design and Fatigue Analysis of Epicyclic Gearbox Carrier," *International Journal for Innovative Research in Science & Technology*, vol. 1, no. 12, pp. 329-333, 2015. [Google Scholar] [Publisher Link]

[10] F.K. Choy et al., "Modal Analysis of Multistage Gear Systems Coupled With Gearbox Vibrations," *Journal of Mechanical Design*, vol. 114, no. 33, pp. 486-497, 1992. [CrossRef] [Google Scholar] [Publisher Link]

[11] F.K. Choy, "Analytical and Experimental Study of Vibrations in a Gear Transmission," *AIAA/ SAE/ ASME, 27th Joint Propulsion Conference*, pp. 1-22, 1991. [CrossRef] [Google Scholar] [Publisher Link]

[12] Lee Dong-Hwan, Youn In-Seong, and Cheon Gill-Jeong, "A Study on the Vibrational Characteristics of a Gearbox for Epicyclic Gear Train," *The Korean Society of Mechanical Engineers*, pp. 837-842, 2000. [Google Scholar] [Publisher Link]

[13] Hyung-Woo Lee, Dong-Hwan Lee, and No-Gill Park, "An Analytical Investigation on Vibrational Characteristics of Turbo Compressor," *Journal of the Korean Society for Noise and Vibration Engineering*, vol. 8, no. 6, pp. 1069-1077, 1998. [Google Scholar] [Publisher Link]